J|A|C|S
ARTICLES
Published on Web 11/19/2002

Tuning Intermolecular Attraction to Create Polar Order and One-Dimensional Nanostructures on Surfaces

Thuc-Quyen Nguyen, Mark L. Bushey, Louis E. Brus, and Colin Nuckolls*

Contribution from the Department of Chemistry, Columbia University, New York, New York 10027

Received September 12, 2002

Abstract: This study utilizes atomic force microscopy and electrostatic force microscopy to investigate the orientation of overcrowded aromatics in films with submonolayer coverage. The results demonstrate that the side chains in the molecules can be used as a tool to control the molecular order and orientation in thin films. For molecules that do not self-associate well, the interaction with the substrate dominates, and the molecules orient with their aromatic planes parallel to the surface. These monolayers have measurable polar order. For molecules that self-associate well, the opposite orientation is observed. These films are comprised of isolated stacks of molecules parallel to the surface.

Introduction

Measurable polar order is a highly desirable attribute that is responsible for many useful properties such as piezo-, pyro-, and ferroelectricity. Creating spontaneously polar materials on nanometer length scales[1−6] is an important challenge that requires finding alternatives to the poling fields used to align the dipoles of bulk materials.[7] The molecules shown in Figure 1A consist of benzene rings with alternating amide and alkoxyl substituents. These molecules were recently shown to self-assemble through a combination of hydrogen bonds and $\pi-\pi$ interactions into regular cylinders.[8] Because the crowding on the central ring positions the amides out of the ring plane, each monomer should have a dipole moment that could sum as the molecules stack in one-dimensional superstructures (Figure 1B).[9]

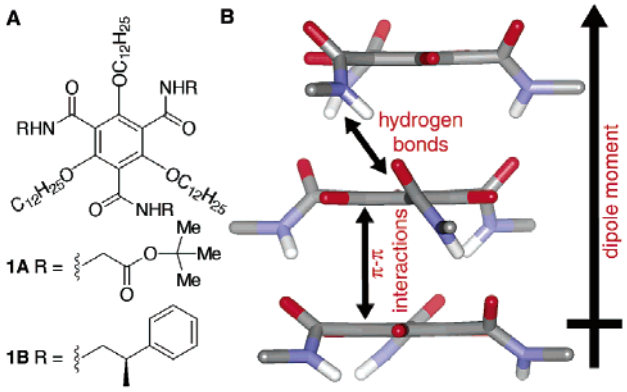

Figure 1. (A) Mesogens **1A**,**B**. (B) Dipolar stacks of **1**.

The study below shows the assembly characteristics and polar properties of **1A** and **1B** in mono- and multilayers using scanning probe microscopy. For **1A**, the molecules prefer the *face-on orientation* with the aromatic rings parallel to the surface in monolayers, and the films are uniformly polar and negatively charged. For **1B**, the molecules preferentially form one-dimensional nanostructures − the *edge-on orientation* − that in some cases consist of isolated molecular stacks parallel to the surface.

Results and Discussion

For this study, atomic force microscopy (AFM) and electrostatic force microscopy (EFM) were utilized to simultaneously measure topography and polarity of monolayer and multilayer films of **1A**,**B**.[10] EFM measures the long-range electrostatic attraction between a conductive AFM cantilever and a conductive substrate. A schematic of the EFM setup is shown in Figure

* To whom correspondence should be addressed. E-mail: cn37@columbia.edu.

(1) (a) Kim, O.-K.; Choi, L.-S.; Zhang, H.-Y.; He, X.-H.; Shih, Y.-H. *Thin Solid Films* **1998**, *327*−*329*, 172−175. (b) Kanazawa, A.; Ikeda, T.; Abe, J. *J. Am. Chem. Soc.* **2001**, *123*, 1748−1754. (c) Kanazawa, A.; Ikeda, T.; Abe, J. *Angew. Chem., Int. Ed.* **2000**, *39*, 612−615.
(2) (a) Bock, H.; Helfrich, W. *Liq. Cryst.* **1992**, *12*, 697−703. (b) Serrette, A. G.; Swager, T. M. *Angew. Chem., Int. Ed. Engl.* **1994**, *33*, 2342−2435. (c) Kilian, D.; Knawby, D.; Athanassopoulou, M. A.; Trzaska, S. T.; Swager, T. M.; Wrobel, S.; Haase, E. *Liq. Cryst.* **2000**, *27*, 509−521. (d) Heiney, P. A.; Fontes, E.; De Jeu, W. H.; Riera, A.; Carroll, P.; Smith, A. B., III. *J. Phys. (Paris)* **1989**, *50*, 461−483. (e) Zheng, H.; Carroll, P. J.; Swager, T. M. *Liq. Cryst.* **1993**, *14*, 1421−1429.
(3) Cresswell, J. P.; Cross, G. H.; Bloor, D.; Feast, W. J.; Petty, M. C. *Thin Solid Films* **1992**, *210*−*211*, 216−218.
(4) (a) Lin, W.; Lin, W.; Wong, G. K.; Marks, T. J. *J. Am. Chem. Soc.* **1996**, *118*, 8034−8042. (b) Beyer, D.; Paulus, W.; Seitz, M.; Maxein, G.; Ringsdorf, H.; Eich, M. *Thin Solid Films* **1995**, *271*, 73−83.
(5) Jaworek, T.; Neher, D.; Wegner, G.; Wieringa, R. H.; Schouten, A. J. *Science* **1998**, *279*, 57−60.
(6) (a) Tew, G. N.; Li, L.; Stupp, S. I. *J. Am. Chem. Soc.* **1998**, *120*, 5601−5602. (b) Pralle, M. U.; Urayama, K.; Tew, G. N.; Neher, D.; Wegner, G.; Stupp, S. I. *Angew. Chem., Int. Ed.* **2000**, *39*, 1486−1489.
(7) Burland, D. M.; Miller, R. D.; Walsh, C. A. *Chem. Rev.* **1994**, *94*, 31−75.
(8) (a) Bushey, M. L.; Hwang, A.; Stephens, P. W.; Nuckolls, C. *J. Am. Chem. Soc.* **2001**, *123*, 8157. (b) Bushey, M. L.; Hwang, A.; Stephens, P. W.; Nuckolls, C. *Angew. Chem., Int. Ed.* **2002**, *41*, 2828−2831.
(9) Similar to the summing of dipole moments in dome-shaped mesogens: (a) Zimmermann, H.; Poupko, R.; Luz, Z.; Billard, J. *Z. Naturforsch., A: Phys., Phys. Chem., Kosmophys.* **1985**, *40A*, 149−60. (b) Malthete, J.; Collet, A. *J. Am. Chem. Soc.* **1987**, *109*, 7544−5. (c) See ref 2.
(10) For example: (a) Terris, B. D.; Stern, J. E.; Rugar, D.; Mamin, H. J. *Phys. Rev. Lett.* **1989**, *63*, 2669. (b) Uchihashi, T.; Okusako, T.; Tsuyuguchi, T.; Sugawara, Y.; Igarashi, M.; Kaneko, R. Morita, S. *Jpn. J. Appl. Phys., Part 1* **1994**, *33*, 5573. (c) de Santo, M. P.; Barberi, R.; Blinov, L. M.; Palto, S. P.; Yudin, S. G. *Mol. Mater.* **2000**, *12*, 329−345.

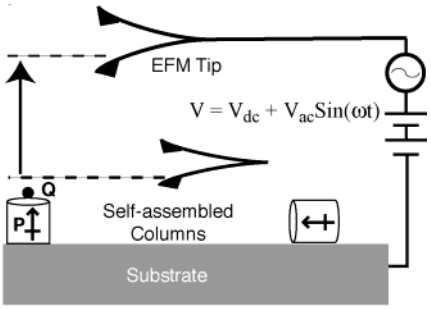

Figure 2. EFM setup for measuring surface charges and permanent dipoles in self-assembled columnar films. Schematic of columns of different polarity interacting with biased EFM tips.

2. Surface charges (Q) and permanent dipoles (P) generate images in the tip by interacting with the total charge on the EFM tip through a Coulombic interaction. The attraction between the cantilever and the substrate is proportional to the square of the voltage difference between them. Thus, application of a sinusoidal voltage $V = V_{dc} + V_{ac}\sin(\omega t)$ yields components of the attractive force at zero frequency, ω and 2ω. The force at ω gives a local measure of Q and P, and the force at 2ω gives information about the dielectric constant of a material.[11] The details of the EFM experiment setup and theory are described elsewhere.[11]

EFM is extremely sensitive, being able to measure a net charge of about 0.1 electron at a distance of 10 nm.[11] Therefore, EFM could potentially detect the difference in dipole moment from columns of opposite polarity. For this study, conditions were found by varying the spin-rate, solvent, and concentration to produce films of **1A** and **1B** on the basal plane of freshly cleaved highly oriented pyrolytic graphite (HOPG) that had less than monolayer coverage.[12] The film morphology is reproducible and always shows drastically different features when comparing **1A** and **1B**. **1A** and **1B** were employed in this study because their associations in bulk were shown previously to be controlled by the constitution of the side chains.[8] Molecular models indicate that stacking **1A** into the idealized structures, such as those in the model in Figure 1B, is difficult because the bulky side chains are encumbering hydrogen bonds between amide substituents. Accordingly, X-ray diffraction and IR spectroscopy have shown that the molecules stack through hydrogen bonds either canted or offset creating a distortion from an idealized hexagonal lattice.[8a] Alternatively, modeling of **1B** shows that its methyl and phenyl substituents in the side chains are able to contact each other to stabilize the structures in Figure 1B.[8b] Supporting this model are the X-ray diffraction and polarized light microscopy results for **1B** that reveal a liquid crystalline phase with a two-dimensional, hexagonal arrangement of columns.[8b]

(11) (a) Krauss, T. D.; O'Brien, S.; Brus, L. E. *J. Phys. Chem. B* **2001**, *105*, 1725. (b) Jiang, J.; Krauss, T. D.; Brus, L. E. *J. Phys. Chem. B* **2000**, *104*, 11936. (c) Cherniavskaya, O.; Chen, L.; Chen, V.; Brus, L. E. *J. Phys. Chem. B*, submitted for publication.

(12) Solutions (between 1 mM and 1 μM) for **1A**,**B** were prepared in anhydrous methylene chloride and then spun onto the basal plane of freshly cleaved HOPG substrates immediately prior to use. The films were dried in air for ~20 min before imaging. Both topographic and EFM images of the films were obtained using a Nanoscope IIIa/MultiMode scanning probe microscope from Digital Instruments. For AFM experiments, etched silicon tips with a typical spring constant of 1−5 N/m and a resonant frequency of 50−80 kHz were used. All AFM images were collected using tapping mode and in air under ambient conditions. For EFM experiments, all measurements were done inside an N_2 purge box with a relative humidity of less than 5% to prevent possible screening effects of a water layer that might absorb on the sample surface. Platinum−iridium coated silicon tips with a spring constant between 1 and 1.3 N/m (NanoSensors) were used for the EFM measurements.

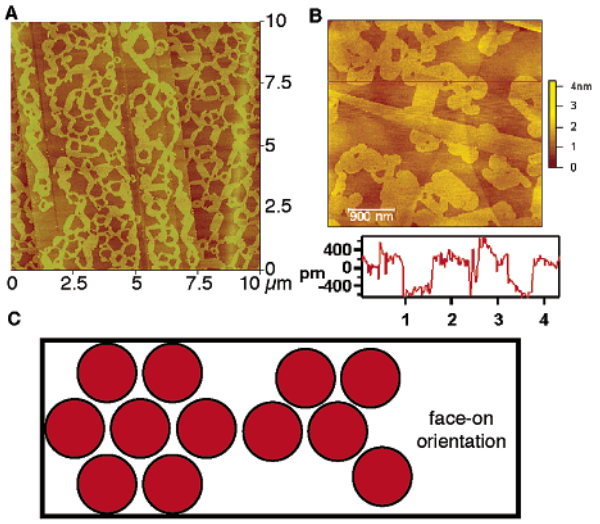

Figure 3. (A) 100 μm^2 AFM image of less than monolayer coverage for **1A** on graphite. (B) Cross-section profile of a submonolayer film of **1A**. (C) Schematic of the "face-on" orientation of **1A** on graphite substrates.

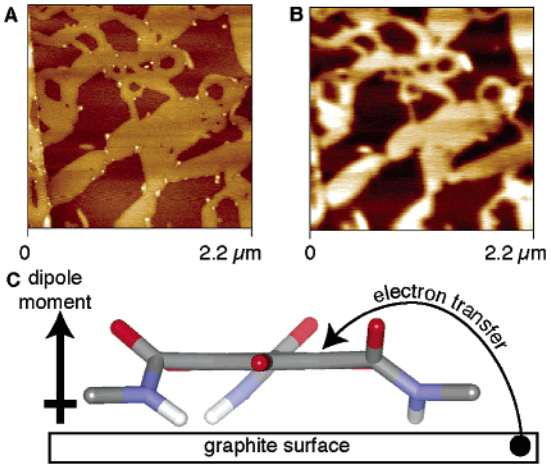

Figure 4. (A) 4.8 μm^2 AFM height image. (B) EFM 1ω image of the same film. (C) Dipole and electron transfer in thin films of **1A**.

Shown in Figure 3A and 4A are AFM images at various scan sizes (1 and 100 μm^2) of a submonolayer film of **1A** on HOPG. The features are uniformly 0.54 ± 0.04 nm high[13] as displayed in the cross section of the topographic image (Figure 3B). This height is consistent with the distance through the aromatic plane (ca. 0.5 nm) but much too small for the diameter of the molecules measured in molecular models and bulk to be ca. 1.8 nm.[8] Presumably, the bulky glycine ester side chains of **1A** decrease the intermolecular attraction relative to the attraction with the graphite surface so that the molecules form two-dimensional, *monolayer* sheets with their aromatic cores parallel to the substrate − *a face-on configuration* (Figure 3C).[14] In the bulk, the liquid crystalline phase from **1A** is comprised of micrometer-sized domains with column growth perpendicular to the surface[8a] − a homeotropic alignment.[15] Possibly, this bulk

(13) The height values are the average of data collected in multiple regions from seven different films.

(14) Similar to the orientation in Langmuir−Blodgett monolayers of amphiphilic coronene derivatives: Lee, M.; Kim, J.-W.; Peleshanko, S.; Larson, K.; Yoo, Y.-S.; Vaknin, D.; Markutsya, S.; Tsukruk, V. V. *J. Am. Chem. Soc.* **2002**, *124*, 9121−9128.

(15) (a) Destrade, C.; Foucher, P.; Gasparoux, H.; Nguyen, H. T.; Levelut, A. M.; Malthete, J. *Mol. Cryst. Liq. Cryst.* **1984**, *106*, 121−146. (b) Billard, J.; Dubois, J. C.; Nguyen, H. T.; Zann, A. *Nouv. J. Chim.* **1978**, *2*, 535−540. (c) Bouligand, Y. *J. Phys. (Orsay, Fr.)* **1980**, *41*, 1307−1315.

arrangement arises from an initial monolayer of molecules, like the one in the Figure 3A, controlling the direction of stacking.[16]

The EFM images of the monolayers formed from **1A** (Figure 4B) trace the same morphology as the height image (Figure 4A). These films have a universal net *negative* charge. The EFM signal is a convolution of the molecular charge (Q) due to charge transfer from the substrate and/or the perpendicular, permanent dipole moment (P). The molecules are dipolar because the amides are forced out of the aromatic plane. The positively charged amide N−H is then in a conformation favorable to form a N−H/π interaction with the graphite substrate (Figure 4C). Effectively, the surface serves to orient the amide substituents and thereby direct the molecular dipoles.[17] Direct evidence for the N−H/π interaction has not been obtained, but similar interactions have been observed between amines and carbon nanotube surfaces.[18] Electron transfer from the graphite to the monolayers is likely also a contributor to the EFM signal (shown in Figure 4C). EFM images of bilayer and trilayer films still retain their net negative charge.

1B was next investigated to see how altering intermolecular interactions affected film formation and column growth. A large area (16 μm^2) AFM image from submonolayer films of **1B** is shown in Figure 5A. The dominant feature in the micrograph is the large number of molecular-scale, fibrous regions. Under optimized conditions varying concentration and spin-casting speed, the fibers formed can be as long as 6 μm. Each of the striations within a fiber is ca. 2 nm in diameter (Figure 5B), and the height of these features is 1.80 ± 0.22 nm (Figure 5C).[19] These values correlate well with the 1.8 nm spacing measured from bulk synchrotron X-ray diffraction.[8b] The implication is that each of the fibers consists of stacks of molecules with the aromatic cores perpendicular to the substrate as shown in Figure 5D. That **1B** preferentially forms long fibers is a direct result of the increased association between subunits from the positive interaction between the side chains.[8b] Performing EFM on these stacks reveals that they have essentially no measurable dipole or charge (Figure 6), consistent with the column axial dipole moment being parallel to the surface (Figure 5D). Moreover, the hydrocarbon exterior insulates these stacks against charge transfer from the substrate. Typically, discotic liquid crystals do not form isolated one-dimensional structures but rather two-dimensional sheets because the relatively weak π-stacking forces holding the column together are nearly equaled by the numerous van der Waals contacts between alkyl side chains.[20] For **1B**, the self-association in the stacking direction outweighs these van der Waals contacts, and isolated stacks for **1B** can form.

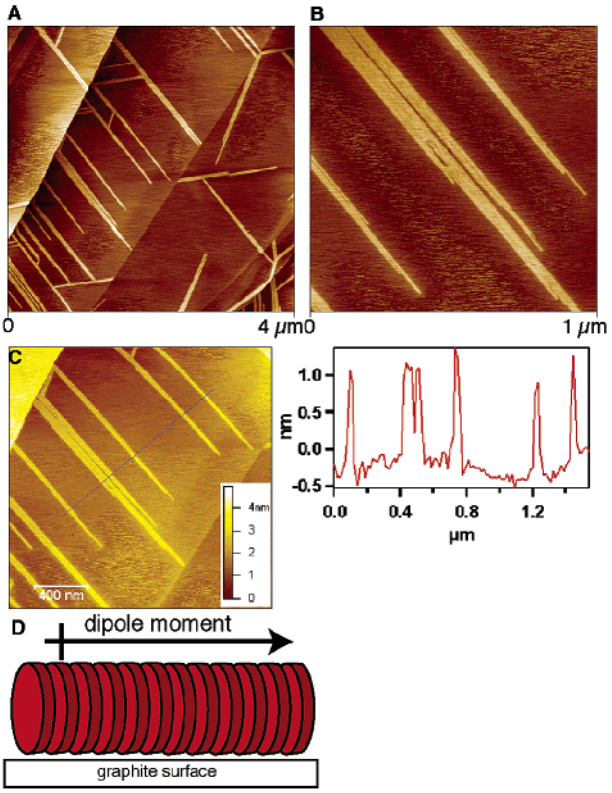

Figure 5. AFM images of **1B** on graphite at various scan sizes: (A) 16 μm^2, (B) 1 μm^2. (C) The cross-section profile of a fiber. (D) Schematic of orientation of **1B** on graphite substrates.

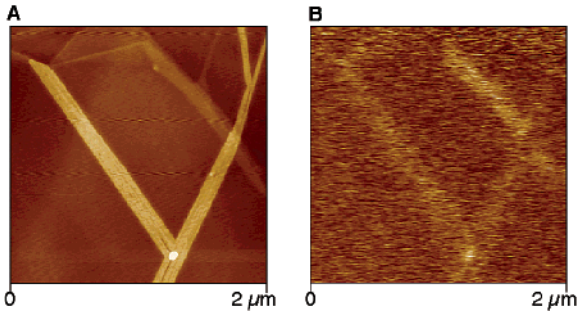

Figure 6. (A) 4 μm^2 AFM height image of less than monolayer coverage for **1B** on graphite. (B) EFM 1ω image of the same film.

Conclusion

In summary, we have demonstrated that we are able to use the side chains of the molecules as a tool to control the molecular order and orientation in thin films of overcrowded aromatics. The data above provide direct imaging of the order and alignment previously seen in bulk samples of **1A** and **1B**.[8a,b] In **1A**, the molecules form monolayers that have a measurable polar order. These monolayers could be useful as a tool to orient the dipole moments of molecules they stack − a hydrogen bond surface template. This could create arrays of polar columns that

(16) An initial monolayer of molecules has been proposed as the mechanism by which the homeotropic alignment results in disc-shaped liquid crystals, see: (a) Vauchier, C.; Zann, A.; Le Barny, P.; Dubois, J. C.; Billard, J. *Mol. Cryst. Liq. Cryst.* **1981**, *66*, 423−433. (b) Schönherr, H.; Kremer, F. J. B.; Kumar, S.; Rego, J. A.; Wolf, H.; Ringsdorf, H.; Jaschke, M.; Butt, H.-J.; Bamberg, E. *J. Am. Chem. Soc.* **1996**, *118*, 13051−13057.

(17) Surface poling has been observed locally in polymer films: Chen, X. Q.; Yamada, H.; Terai, Y.; Horiuchi, T.; Matsushige, K.; Weiss, P. S. *Thin Solid Films* **1999**, *353*, 259−263.

(18) Similar to the recognition of carbon nanotubes with amines: (a) Liu, J.; Casavant, M. J.; Cox, M.; Walters, D. A.; Boul, P.; Lu, W.; Rimberg, A. J.; Smith, K. A.; Colbert, G. T.; Smalley, R. E. *Chem. Phys. Lett.* **1999**, *303*, 125−129. (b) O'Connell, M. J.; Boul, P.; Ericson, L. M.; Huffman, C.; Wang, Y.; Haroz, E.; Kuper, C.; Tour, J.; Ausman, K. D.; Smalley, R. E. *Chem. Phys. Lett.* **2001**, *332*, 461−466. (c) Kong, J.; Dai, H. *J. Phys. Chem. B* **2001**, *105*, 2890−2893. (d) Sano, M.; Kamino, A.; Okamura, J.; Shinkai, S. *Nano Lett.* **2002**, *2*, 531−533.

(19) The height values are the average of data collected in 7−10 regions from three different films.

(20) (a) Henderson, P.; Beyer, D.; Jonas, U.; Karthaus, O.; Ringsdorf, H.; Heiney, P. A.; Maliszewskyj, N. C.; Ghosh, S. S.; Mindyuk, O. Y.; Josefowicz, J. Y. *J. Am. Chem. Soc.* **1997**, *119*, 4740−4748. (b) Maliszewskyj, N. C.; Heiney, P. A.; Josefowicz, J. Y.; McCauley, J. P., Jr.; Smith, A. B., III. *Science* **1994**, *264*, 77−79. (c) Josefowicz, J. Y.; Maliszewskyj, N. C.; Idziak, S. H. J.; Heiney, P. A.; McCauley, J. P., Jr.; Smith, A. B., III. *Science* **1993**, *260*, 323−326. (d) Tsukruk, V. V.; Reneker, D. H.; Bengs, H.; Ringsdorf, H. *Langmuir* **1993**, *9*, 2141−2144. (e) Christ, T.; Geffarth, F.; Glüsen, B.; Kettner, A.; Lüssem, G.; Schäfer, O.; Stümpflen, V.; Wendorff, J. H.; Tsukruk, V. V. *Thin Solid Films* **1997**, *302*, 214.

are perpendicular to the substrate. Experiments are underway to use scanning probe microscopy[21] to determine if these films have properties that are a consequence of their polar order such as pyro-, ferro-, and piezoelectricity. For **1B**, the films have their column axis parallel to the substrate. By further tuning the property of these the aromatic rings, these nanostructures could be used to study electronic transport properties in one-dimensional, organic semiconductors.[22]

Acknowledgment. We thank Jiang Jiang for assistance with the EFM instrument, and Fotios Papadimitrakopoulos and Oksana Cherniavskaya for useful discussions. We acknowledge financial support from the Chemical Sciences, Geosciences, and Biosciences Division, Office of Basic Energy Sciences, U.S. D.O.E. (#DE-FG02-01ER15264) and U.S. National Science Foundation, Nanoscale Exploratory Research Grant (#DMR-01-02467). This work is supported in part by the Nanoscale Science and Engineering Initiative of the National Science Foundation under NSF Award Number CHE-0117752. C.N. thanks the Beckman Young Investigator Program (2002) and the Dupont Young Investigator Program (2002) for financial support. M.L.B. thanks the ACS Division of Organic Chemistry for a graduate fellowship sponsored by Bristol-Myers Squibb.

JA028524H

(21) (a) Labardi, M.; Likodimos, V.; Allegrini, M. *Phys. Rev. B* **2000**, *61*, 14391−14398. (b) Luethi, R.; Haefke, H.; Meyer, K. P.; Meyer, E.; Howald, L.; Guentherodt, H. J. *J. Appl. Phys.* **1993**, *74*, 7461−7471. (c) Christman, J. A.; Woolcott, R. R.; Kingon, A. I.; Nemanich, R. J. *Appl. Phys. Lett.* **1998**, *73*, 3851−3853. (d) Ganpule, C. S.; Nagarajan, V.; Ogale, S. B.; Roytburd, A. L.; Williams, E. D.; Ramesh, R. *Appl. Phys. Lett.* **2000**, *77*, 3275−3277. (e) Kuffer, O.; MaggioAprile, I.; Triscone, J. M.; Fischer, O. *Appl. Phys. Lett.* **2000**, *77*, 1701−1703. (f) Durkan, C.; Chu, D. P.; Migliorato, P.; Welland, M. E. *Appl. Phys. Lett.* **2000**, *76*, 366−368.

(22) (a) Adam, D.; Schuhmacher, P.; Simmerer, J.; Haeussling, L.; Siemensmeyer, K.; Etzbach, K. H.; Ringsdorf, H.; Haarer, D. *Nature* **1994**, *371*, 141−143. (b) Boden, N.; Bushby, R. J.; Clements, J.; Luo, R. *J. Mater. Chem.* **1995**, *5*, 1741−1748. (c) Boden, N.; Bushby, R. J.; Clements, J. *J. Chem. Phys.* **1993**, *98*, 5920−5931. (d) Boden, N.; Borner, R. C.; Bushby, R. J.; Clements, J. *J. Am. Chem. Soc.* **1994**, *116*, 10807−10808. (e) van de Craats, A. M.; Warman, J. M.; Fechtenkotter, A.; Brand, J. D.; Harbison, M. A.; Müllen, K. *Adv. Mater.* **1999**, *11*, 1469.